Sliding Mode Based Virtual Sensor for Feedback Linearization in Delta Robots with Unknown Dynamic Model

Iyad Hashlamon
Department of Mechanical Engineering, Palestine Polytechnic University
Hebron, Palestine, iyad@ppu.edu

***Abstract*-- Delta robots are of nonlinear dynamics, therefore applying linear controllers to satisfy the required trajectory tracking is a challenge which becomes more significant when the robot model is unknown. This paper proposes a stable virtual sensor to be used for feedback linearization for delta robots with unknown dynamic model. The sensor design is based on the second order sliding mode observer. This sensor considers that only the inertia of the robot upper links with the motor inertia are known. As a measurement, only the active joints position angles are measured. The stability is proven using Lyapunov theory and explicit relations for the design parameters are obtained. To overcome the effect of the transient response of this sensor, an adaptive tuning gain with maximum value of unity is introduced in the feedback to improve the compensation performance. The results validate this sensor and prove its dramatic performance improvement in trajectory tracking when combined with the PD controller.**

***Index Term*-- Delta robot, sliding mode observer, disturbance estimation, adaptive control, virtual sensor.**

1. INTRODUCTION

Virtual sensors are considered to be software sensors that use measured variables in relatively simple models, they are used in several applications [1-5]. The use of these sensors increases the measurement redundancy and reliability of the measurement systems and overcomes the hardware size and cost limitations [6, 7]. Further, virtual sensors can be used in systems with unknown models as in this paper.

Trajectory tracking using classical control approaches is reported [8, 9 , 10-12]. However, unmodeled dynamics and disturbances deteriorate the controller performance[13]. Neglecting the coupling effects is the design principle in Proportional–derivative (PD) and Proportional- integral derivative PID controllers used to control delta robots[14], this requires improving the tracking errors [15]. Recent nonlinear PD with sliding mode control was reported in [16], however, sliding mode controller's major problem is chattering. The research on adaptive control of delta robot is still ongoing [17] to restrain model uncertainties problems.

Obtaining linearized model via feedback linearization simplifies the application of linear controllers using linear pole placement techniques [18, 19], it assumes that the exact dynamic model is obtained and available. However, it becomes more challenging when the robot model is partially known or unknown like the case in this paper. Sliding mode observers are employed here to overcome this challenge.

The sliding mode observers are characterized by the finite-time convergence and robustness to uncertainties [20]. Generally the observer is designed by injecting a nonlinear discontinuous term. This injector must be designed to force the system trajectories to remain on the a sliding surface in the error space, this results in disturbance rejection [21]. First order sliding mode observers are restricted to systems with output relative degree of one and may cause chattering [22]. Higher order sliding modes can improve the first order sliding mode observers [23]. The second order sliding mode observer with twisting algorithm is studied in [20], the stability analysis is based on the majorant curve. The author in [24] studied the stability and convergence based on Lyapunov function.

This paper contributes in proposing a virtual sensor which is designed based on a second order sliding mode observer for delta robots with unknown dynamic model. It is considered that only the active joint position is measured, and the model is unknown except the constant diagonal matrix that represents the inertia of the links and the motors. The inertia matrix, Coriolis and centrifugal torques, gravitational terms acting on the robot and joint friction are unknown and considered as lumped disturbance vector to be estimated. The stability is proven based on Lyapunov theory. This leads to obtain explicit relations for the design parameters. An adaptive tuning gain surface is developed based on the error between the actual and desired joint angles. This gain scales the estimated disturbance adaptively to overcome the overshoot at the beginning of the estimation process. The tuned disturbance is added to the control signal of a designed PD controller to study the tracking trajectory performance.

The rest of the paper is organized as follows: the delta robot model is in section 2, section 3 introduces the problem statement, the virtual sensor design is in section 4. Section 5 shows the control approach, section 6 discusses the results, the paper is concluded in section 7.

2. DELTA ROBOT

The schematic of the three degree of freedom (3-DoF) delta robot is shown in Fig. 1. The robot structure is composed of fixed plate, three active revolute joints and links, three passive links and the moving platform.

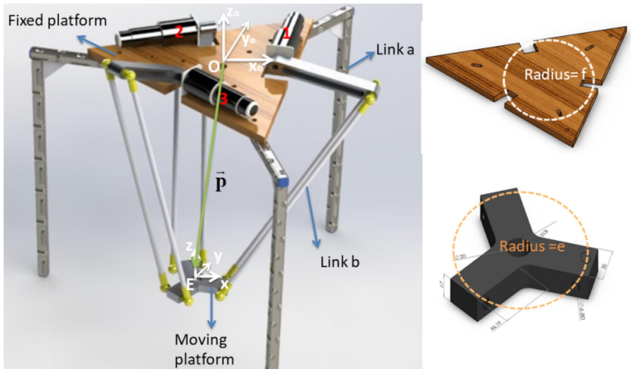

Fig. 1. Delta robot

The kinematics and dynamics models of the robot are well explained in the literature, e.g. see [25-32]. The Delta robot is described by the differential equations as

$$M(\boldsymbol{\theta})\ddot{\boldsymbol{\theta}} + C(\boldsymbol{\theta},\dot{\boldsymbol{\theta}})\dot{\boldsymbol{\theta}} + G(\boldsymbol{\theta}) + \boldsymbol{\tau}_{\mathbf{F}} = \boldsymbol{\tau} \ , \qquad (1)$$

where $\boldsymbol{\theta} = \begin{bmatrix} \theta_1 & \theta_2 & \theta_3 \end{bmatrix}^T \in \mathbb{R}^3$ is the set of the actuated joints vector. $\boldsymbol{\theta}$ is measured using joint encoders attached to the joint actuators . $M \in \mathbb{R}^{3\times3}$ is the positive definite inertia matrix, $C\left(\boldsymbol{\theta},\dot{\boldsymbol{\theta}}\right)\dot{\boldsymbol{\theta}} \in \mathbb{R}^3$ vector represents the Coriolis and centrifugal torques, $G\left(\boldsymbol{\theta}\right) \in \mathbb{R}^3$ contains the gravitational terms acting on the robot, $g = 9.81 m/s^2$ is the gravity constant, $\boldsymbol{\tau}_{\mathbf{F}} \in \mathbb{R}^3$ is the joint frictional vector and $\boldsymbol{\tau} \in \mathbb{R}^3$ is the generalized joint control vector. The above terms include the moving plate position $\mathbf{p} \equiv \begin{bmatrix} p_x & p_y & p_z \end{bmatrix}^T$ in $\mathbb{R}^3$. The link a has length L_a and mass m_a . The link b has length L_b and mass m_b . The fixed platform has the frame O and radius f , the moving platform has radius e and mass m_p with the frame E parallel to the fixed platform frame O as shown in Fig. 1. The actuators are considered identical with inertia $\mathbf{I}_m$ and gear ratio k_m . The elbow joint has a mass m_e . Each link a_i for $i = 1,2,3$ is rotated an angle α around the axis z_o in the frame O. Accordingly, $\alpha_1 = 0^o, \alpha_2 = 120^o$ and $\alpha_3 = 240^o$ with the rotation matrix

$${}^{i}R_{z_o}(\alpha_i) = \begin{bmatrix} \cos(\alpha_i) & -\sin(\alpha_i) & 0 \\ \sin(\alpha_i) & \cos(\alpha_i) & 0 \\ 0 & 0 & 1 \end{bmatrix}.$$

The inertia of motors with the upper links $\mathbf{I}$ is represented by

$$\mathbf{I} = k_m^2 \mathbf{I}_m + L_a^2 \left(\frac{m_a}{3} + m_e + \frac{2}{3} m_b \right) I_3$$

where I_3 is the identity matrix of size three. Then the matrices in Eq (1) M , C and G are given as

$$M = \left(m_p + m_b\right) J^T J + \mathbf{I} \ , \qquad C = J^T \left(m_p + m_b\right) \dot{J} \qquad \text{and}$$

$$G = \left[-J^T \left(m_p + m_b\right) \begin{bmatrix} 0 \\ 0 \\ -g \end{bmatrix} - \gamma m g \begin{bmatrix} \cos\theta_1 \\ \cos\theta_2 \\ \cos\theta_3 \end{bmatrix} \right] \quad \text{respectively with}$$

$m = m_a + m_e + \frac{2}{3} m_b$ and $\gamma = \frac{\frac{1}{2} m_a + m_e + \frac{2}{3} m_b}{m} L_a$. J and $\dot{J}$ represent the Jacobian and its time derivative respectively. The Jacobian is a function of both the actuated angles θ_i and the position of the end effector which is found using the forward kinematics. For more details refer to [28] .

3. PROBLEM DEFINITION AND FORMULATION

In general, for known dynamic model, feedback linearization with PD controller will achieve the desired transient and steady state response for a manipulator by using simple linear pole placement techniques [33]. However, it is not always the case were the dynamic models are known and there is no disturbance, further, the system parameters may change due the environment and time such as joint friction [34, 35].

This paper considers that the delta robot dynamic model is unknown and it is controlled using PD controller with feedback linearization. It considers that only the constant diagonal matrix $\mathbf{I}$ is known. In other words, the inertia matrix is written as $M(\boldsymbol{\theta}) = \mathbf{I} + \tilde{M}(\boldsymbol{\theta})$ where $\tilde{M}$ is the uncertainty in M .

For the system in Eq (1), define the states $\mathbf{x}_1 = \begin{bmatrix} \theta_1 & \theta_2 & \theta_3 \end{bmatrix}^T$ and $\dot{\mathbf{x}}_1 \equiv \mathbf{x}_2 = \begin{bmatrix} \dot{\theta}_1 & \dot{\theta}_2 & \dot{\theta}_3 \end{bmatrix}^T$, then Eq (1) can be written in state space representation as

$$\begin{aligned} \dot{\mathbf{x}}_1 &= \mathbf{x}_2 \\ \dot{\mathbf{x}}_2 &= M^{-1}(\mathbf{x}_1)\left(\boldsymbol{\tau} - C\left(\mathbf{x}_1, \mathbf{x}_2\right)\mathbf{x}_2 - G(\mathbf{x}_1) - \boldsymbol{\tau}_{\mathbf{F}}\right) \qquad (2) \\ y &= \mathbf{x}_1 \end{aligned}$$

where $\mathbf{x}_1$ is the measured robot actuated joints position. Let all the uncertain terms be combined as lumped nonlinear disturbance vector called $\zeta \equiv [\zeta_1 \quad \zeta_2 \quad \zeta_3]^T$, then Eq (2) can be rewritten as

$$\begin{aligned} \dot{\mathbf{x}}_1 &= \mathbf{x}_2 \\ \dot{\mathbf{x}}_2 &= \mathbf{I}^{-1}\boldsymbol{\tau} + \overline{\zeta} \\ y &= \mathbf{x}_1 \end{aligned} \quad , \tag{3}$$

where $\overline{\zeta} = \mathbf{I}^{-1}\zeta$ and ζ is given by

$$\begin{aligned} \zeta &= -\left(C(\boldsymbol{\theta},\dot{\boldsymbol{\theta}})\dot{\boldsymbol{\theta}} + G(\boldsymbol{\theta}) + \boldsymbol{\tau}_{\mathbf{F}} - \tilde{M}(\boldsymbol{\theta})\ddot{\boldsymbol{\theta}}\right) \\ &= -\left(C(\mathbf{x}_1,\mathbf{x}_2)\mathbf{x}_2 + G(\mathbf{x}_1) + \boldsymbol{\tau}_{\mathbf{F}} - \tilde{M}(\mathbf{x}_1)\dot{\mathbf{x}}_2\right) \end{aligned} \quad , \tag{4}$$

The paper will show the design of a virtual disturbance sensor for the original system in Eq (1), when only the position vector $\boldsymbol{\theta} \equiv \mathbf{x}_1$ for the three joints is measured. The joints angular velocity vector $\dot{\boldsymbol{\theta}} \equiv \mathbf{x}_2$ is to be observed. The proposed method does not require the calculation of the M, C and G matrices in Eq (2). Therefore the Jacobian calculation is avoided.

The stability proof is based on Lyapunov approach. The solutions to the system in Eq (3) are in the sense of Filippov [24].

4. Virtual Sensor Design Based on Sliding Mode

Consider the super twisting observer of the form

$$\begin{aligned} \dot{\hat{\mathbf{x}}}_1 &= \hat{\mathbf{x}}_2 + \mathbf{z}_1 \\ \dot{\hat{\mathbf{x}}}_2 &= \mathbf{I}^{-1}\boldsymbol{\tau} + \mathbf{z}_2 \end{aligned} \tag{5}$$

where $\hat{\mathbf{x}}_1$ and $\hat{\mathbf{x}}_2$ are the state estimation of the real states $\mathbf{x}_1$ and $\mathbf{x}_2$ respectively. $z_i, i = 1,2$ are the observer injectors and used to eliminate the error between the estimated states and the actual states. They are defined as

$$\begin{aligned} \mathbf{z}_1 &= \lambda_1 |\tilde{\mathbf{x}}_1|^{\frac{1}{2}} sign(\tilde{\mathbf{x}}_1) \\ \mathbf{z}_2 &= \lambda_2 |\tilde{\mathbf{x}}_1|^{\frac{1}{2}} sign(\tilde{\mathbf{x}}_1) \end{aligned} \tag{6}$$

where $\tilde{\mathbf{x}}_1$ is the error and expressed as $\tilde{\mathbf{x}}_1 = \mathbf{x}_1 - \hat{\mathbf{x}}_1$. λ_1 and λ_2 are the observer gains. Define $\tilde{\mathbf{x}}_2 = \mathbf{x}_2 - \hat{\mathbf{x}}_2$, then the error dynamics are

$$\begin{aligned} \dot{\tilde{\mathbf{x}}}_1 &= \tilde{\mathbf{x}}_2 - \mathbf{z}_1, \\ \dot{\tilde{\mathbf{x}}}_2 &= \overline{\zeta} - \mathbf{z}_2, \end{aligned} \tag{7}$$

For this robot, the actuator angular motion is bounded. Thus, it is assumed that the states are bounded and there is a positive constant $\boldsymbol{\rho}$ such that

$$|\overline{\zeta}| < \boldsymbol{\rho} \tag{8}$$

holds for $\mathbf{x}_1$ and $\hat{\mathbf{x}}_2$ for all time t. The structure of the virtual sensor is shown in Fig. 2.

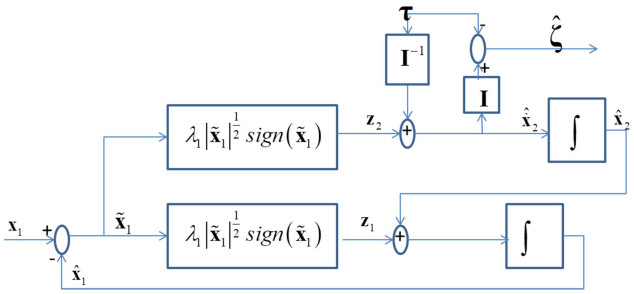

Fig. 2. Virtual sensor main structure

Theorem: for the given system in Eq (3) and the observer in Eq (5), the estimated states $\hat{\mathbf{x}}$ will converge to the real states $\mathbf{x}$ if the condition in Eq (8) holds and the observer gains are selected as

$$\begin{aligned} \lambda_1 &= diag(\lambda_{11}, \lambda_{12}, \lambda_{13}) \\ \lambda_2 &= diag(\lambda_{21}, \lambda_{22}, \lambda_{23}) \end{aligned} \tag{9}$$

where $diag$ stands for diagonal matrix, $(\lambda_{11}, \lambda_{12}, \lambda_{13}) > 0$ and $\lambda_{2i} > \dfrac{\rho\lambda_{1i}^2 + 2\rho^2}{\lambda_{1i}^2}$ for $i = 1,2,3$.

Proof: to prove this theorem, it is important to show that the error $\tilde{\mathbf{x}}_1$ and $\dot{\tilde{\mathbf{x}}}_1$ converge to zero. i.e. $\tilde{\mathbf{x}}_1, \dot{\tilde{\mathbf{x}}}_1 \to 0$. For sake of simplicity, only the scalar case $x_1, x_2 \in \mathbb{R}$ is considered, λ_1 and λ_2 are considered to be scalar too. The proof depends on the Lyapunov approach.

Consider the strong Lyapunov function $V(\tilde{x})$ [24]

$$V(\tilde{x}_1, \tilde{x}_2) = 2\lambda_2 |\tilde{x}_1| + \frac{1}{2}\tilde{x}_2^2 + \frac{1}{2}\left(\lambda_1 |\tilde{x}_1|^{1/2} sign(\tilde{x}_1) - \tilde{x}_2\right)^2 \tag{10}$$

Or in matrix from

$$V(\tilde{x}) = \Upsilon^T R \Upsilon \tag{11}$$

Where $\Upsilon = \left[|\tilde{x}_1|^{1/2} sign(\tilde{x}_1) \quad \tilde{x}_2\right]^T$ and

$$R = \frac{1}{2}\begin{bmatrix} 4\lambda_2 + \lambda_1^2 & -\lambda_1 \\ -\lambda_1 & 2 \end{bmatrix}$$

This function is continuous everywhere and not differentiable at $\tilde{x}_1 = 0$. Therefore, a nonsmooth version of Lyapunov theory is required [36]. Further, the identity $d|x|/dt = \dot{x}\,\mathrm{sign}\,x$ is used here. Since $V(0,0) = 0$ then the point $\tilde{x}_1 = 0$ and $\tilde{x}_2 = 0$ is an equilibrium point. Further,

$V(\tilde{x}_1,\tilde{x}_2)>0$ for $\lambda_2>0$. The time derivative of Eq (11) is given by

$$\dot{V}(\tilde{x}_1,\tilde{x}_2)=-\frac{1}{|\tilde{x}_1|^{1/2}}\Upsilon^T Q_1\Upsilon+\Upsilon^T Q_2\Upsilon+\zeta\begin{bmatrix}-\lambda_1 & 2\end{bmatrix}\Upsilon \tag{12}$$

where

$$Q_1=\begin{bmatrix}2\lambda_1\lambda_2+\frac{\lambda_1^3}{2} & -2\lambda_2\\ -\lambda_1^2 & \frac{\lambda_1}{2}\end{bmatrix}$$

and

$$Q_2=\begin{bmatrix}\lambda_1\lambda_2 & -\lambda_2\\ -\lambda_2 & 0\end{bmatrix}.$$

Applying the bound in inclusion in Eq (8), Eq (12) can be written as

$$\dot{V}(\tilde{x}_1,\tilde{x}_2)<-\frac{1}{|\tilde{x}_1|^{1/2}}\Upsilon^T\tilde{Q}_1\Upsilon \tag{13}$$

with

$$\tilde{Q}_1=\frac{\lambda_1}{2}\begin{bmatrix}2\lambda_2+\lambda_1^2+2\rho & -\lambda_1-\frac{2\rho}{\lambda_1}\\ -\lambda_1-\frac{2\rho}{\lambda_1} & 1\end{bmatrix}$$

For the stability and convergence to the equilibrium point, it is required that $\dot{V}(\tilde{x}_1,\tilde{x}_2)$ to be negative definite. This condition is satisfied if the matrix $\tilde{Q}_1$ is positive definite. The matrix $\tilde{Q}_1>0$ if

$$2\lambda_2+\lambda_1^2+2\rho>\left(-\lambda_1-\frac{2\rho}{\lambda_1}\right)^2, \tag{14}$$

Hence selecting

$$\lambda_1>0$$
$$\lambda_2>\frac{\rho\lambda_1^2+2\rho^2}{\lambda_1^2} \tag{15}$$

Guarantees that $\tilde{Q}_1$ is positive definite and $\dot{V}(\tilde{x}_1,\tilde{x}_2)$ is negative definite. Thus the trajectories converges to the equilibrium point. □

Equation (15) is then extended for the three equations and written as in Eq (9).It follows that the estimated disturbance $\hat{\zeta}$ is

$$\hat{\zeta}=\mathbf{I}\dot{\hat{\mathbf{x}}}_2-\boldsymbol{\tau} \tag{16}$$

Which is the output of the virtual sensor.

5. Control Approach

As mentioned earlier, once the estimated lumped disturbance vector $\hat{\zeta}$ converged to the true value of ζ, i.e. $\zeta-\hat{\zeta}\to 0$, then the model becomes a linearized model where simple linear pole placement techniques can be used to design a controller. A PD controller is designed to track the reference trajectory according to Eq (3) where the error dynamics is given as

$$\ddot{\mathbf{e}}+k_d\dot{\mathbf{e}}+k_p\mathbf{e}=0\ , \tag{17}$$

where $\mathbf{e}=\mathbf{x}_1-\mathbf{x}_{1d}\equiv\begin{bmatrix}e_1 & e_2 & e_3\end{bmatrix}^T$, $\mathbf{x}_{1d}$ is the desired trajectory vector, k_p and k_d are the positive gains of the PD controller which can be determined using pole placement technique.

For the feedback linearization as in Fig. 3, the estimated disturbance is added directly to the PD controller output. However, the estimation has the drawback of the overshoot. To overcome this limitation, the estimated disturbance is adaptively tuned according to the error $\mathbf{e}$ and the maximum allowable error in the system $\mathbf{e}_{\max}\equiv\begin{bmatrix}e_{1_{\max}} & e_{2_{\max}} & e_{3_{\max}}\end{bmatrix}^T$. The tuning gain range is $k_i\in(0,1], i=1,2,3$ and given by

$$k_i=-\frac{1-k_{t_i}}{e_{i_{\max}}}|e_i|+1 \tag{18}$$

where k_{t_i} is a positive number with the inclusion $0<k_{t_i}<1$. Thus the control law is the PD controller output τ_{PD} and the tuned disturbance and given by $\tau_{PD}+k\hat{\zeta}$ with $k=diag(k_1,k_2,k_3)$.

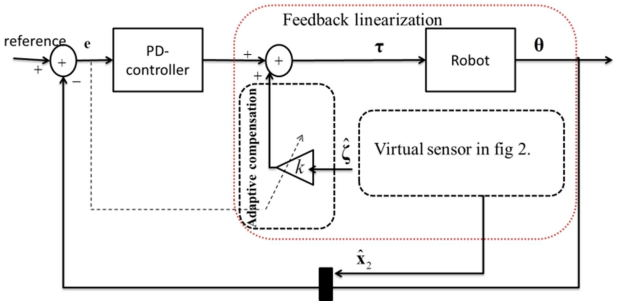

Fig. 3:Adaptive feedback linearization and control of delta robot

6. RESULTS

MATLAB environment is used as an experimental platform to carry out simulations on the robot model. To be more realistic, Gaussian noise was added using MATLAB Simulink Gaussian noise generator with zero mean and variance 0.001. The sampling time of this simulation T=1 ms. The original nonlinear model of the robot is used throughout the simulation. The friction was generated using the function [37]

$$\boldsymbol{\tau}_{\mathbf{F}} = \gamma_1\left(\tanh\left(\gamma_2\dot{\boldsymbol{\theta}}\right)-\tanh\left(\gamma_3\dot{\boldsymbol{\theta}}\right)\right)+\gamma_4\tanh\left(\gamma_5\dot{\boldsymbol{\theta}}\right)+\gamma_6\dot{\boldsymbol{\theta}}$$

where $\gamma_i, i=1,\cdots,6$ are positive constants. The model has the viscous dissipation term $\gamma_6\dot{\boldsymbol{\theta}}$, the Stribeck effect term $\tanh\left(\gamma_2\dot{\boldsymbol{\theta}}\right)-\tanh\left(\gamma_3\dot{\boldsymbol{\theta}}\right)$, the static coefficient of friction $\gamma_1+\gamma_4$ and the coulomb friction $\gamma_4\tanh\left(\gamma_5\dot{\boldsymbol{\theta}}\right)$. The friction model constants are in Table I.

Table I: Friction model paramters

	θ_1	θ_2	θ_3
γ_1	0.7	0.6	5
γ_2	10	10	10
γ_3	10	10	10
γ_4	0.6	0.5	0.4
γ_5	50	100	10
γ_6	0.9	0.9	0.9

The robot parameters are given in Table II.

Table II: Robot parameters

Description	Symbol	Unit
Length of the upper arm	L_a	0.18m
Length of the lower arm	L_b	0.435m
Radius of the base platform	f	0.1m
Radius of the moving platform	e	0.055m
Mass of the upper arm	m_a	0.190Kg
Mass of the lower arm	m_b	0.055 Kg
Mass of the moving platform	m_p	0.196Kg
Gravity acceleration	g	-9.8 m/s^2
Elbow mass	m_e	0.024 Kg
Motor inertia	$\mathbf{I}_m$	81.6×10^{-3}; Kg.m^2
Gear ratio constant	k_m	0.01

The observer parameters are selected to be $\rho=100$, $\lambda_{1i}=50$ and $\lambda_{2i}=5000$ for $i=1,2,3$. The adaptive gain parameters are selected as: $\mathbf{e}_{\max}=[1 \quad 1 \quad 1]$ and $k_{t_i}=0.1$ for $i=1,2,3$. The used PD controller has the transfer function

$$PD(s)=k_p+k_dN\frac{s}{s+N}, \tag{19}$$

with $k_p=25I_3$, $k_d=I_3$ and N=100. s refers to Laplace transform.

Define the disturbance estimation error $\tilde{\xi}$ as $\tilde{\xi}=\hat{\xi}-\xi$. where ξ is the true value generated using the true model with the friction, $\hat{\xi}$ is the estimated value. The aim is that $\tilde{\xi}\to0$ in finite time which is depicted in Fig. 4. However, before the convergence, the oscillations in the transient response affect the control low adversely, the significant effect is when the initial conditions are far from the correct one. Here the initial conditions for the observer are given to be 0.5 for the position and zero for the angular velocity. This can be shown in the phase portrait in Fig. 5 for the first state. The initial position error is at -0.5. Since the error is negative, the velocity error must be positive in order to drive $\tilde{x}_1$ to zero. Once $\tilde{x}_1\to0$, $\dot{\tilde{x}}_1\equiv\tilde{x}_2$ trajectory intersects with the point $\left(0,\tilde{x}_2>0\right)$. Then the trajectory inters the half-plane $\tilde{x}_1>0$, this trajectory is concave down with a conclusion of $\ddot{\tilde{x}}_1\equiv\dot{\tilde{x}}_2<0$ which explains driving the velocity error to zero. The same discussion goes when $\tilde{x}_1>0$ and $\dot{\tilde{x}}_1\equiv\tilde{x}_2<0$ until the trajectory reaches the equilibrium point at $\left(\tilde{x}_1,\dot{\tilde{x}}_1\equiv\tilde{x}_2\right)=(0,0)$ and remains there.

The trajectory tracking response without disturbance compensation as depicted in Fig. 6 is based on the selected PD controller parameters. This figure shows the error between the desired and the actual trajectories and how the response starts from its initial position at the origin point in the $x-y$ plane to track the desired trajectory. On the other hand, the response with disturbance compensation is depicted in Fig. 7 for the same controller and conditions. It shows that the tracking error converges to zero.

Although Fig. 4 shows the quality of the estimated disturbance, however, the transient estimation response affects the control law diversely. Therefore the tuning gain k is used with the aforementioned parameters. The gain k values are changing as in Fig. 8. The maximum value of this

gain is one, i.e. at the steady state this gain has no effect and the same estimated disturbance is added to the controller output. In the transient period, this gain has an important role in terms of decreasing the effect of the estimated disturbance on the control law.

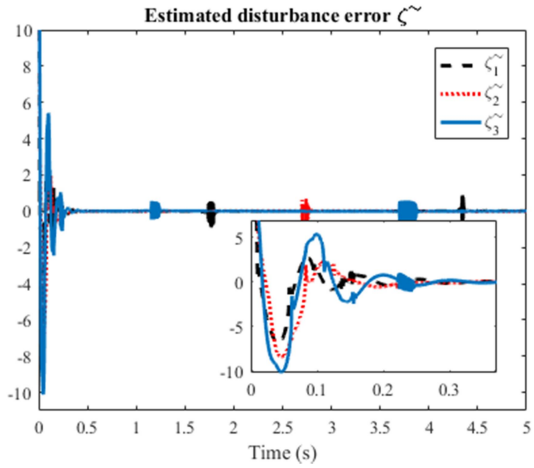

Fig. 4. Disturbance estimation error

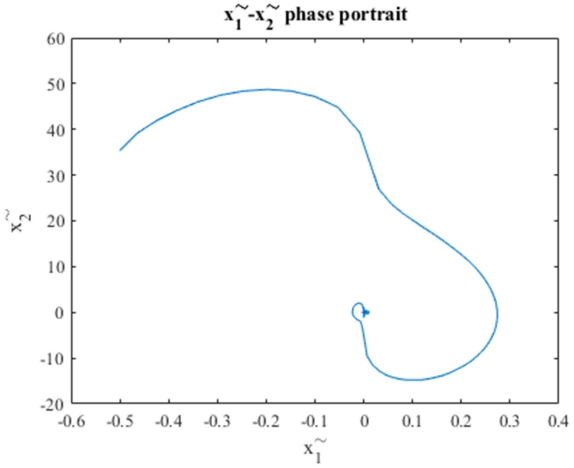

Fig. 5. Phase portrait

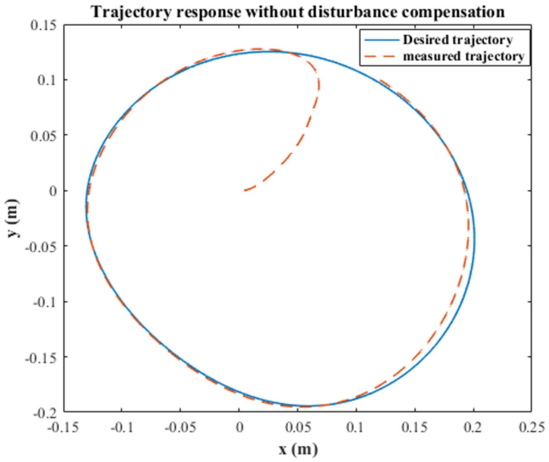

Fig. 6. Trajectory response without disturbance compensation.

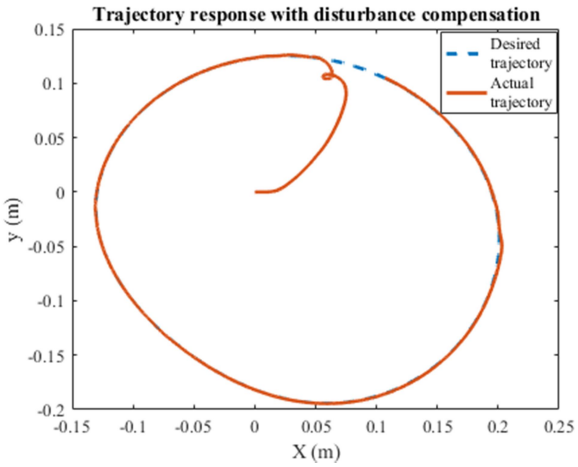

Fig. 7. Trajectory response with disturbance compensation

As can be read from Fig. 8, at the initial run, $e_2 > e_3 > e_1$. As shown the gain for ζ_1 starts with value of larger than 0.8 in the period of the transient response of the estimated disturbance. This indicates that the estimated disturbance $\hat{\zeta}_1$ has more effect on the control law than $\hat{\zeta}_3$ in the transient response. In the same way, $\hat{\zeta}_3$ has more effect on the control law than $\hat{\zeta}_2$ in the transient response. In the control context, this adaptively tuned gain can be used to increase the speed of convergence by changing the values of its parameters that will increase the gain k. However, this costs overshoot and oscillated response as in Fig. 9.

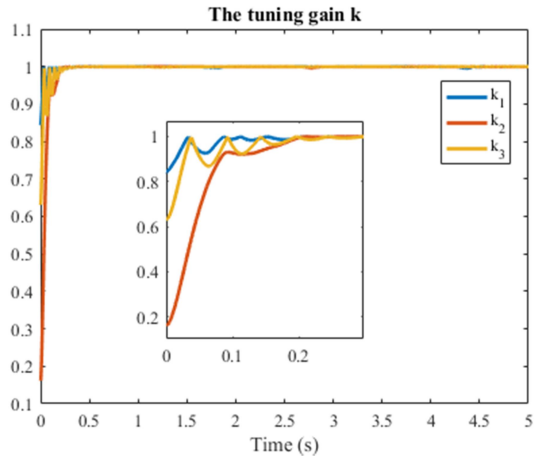

Fig. 8. The tuning gain values

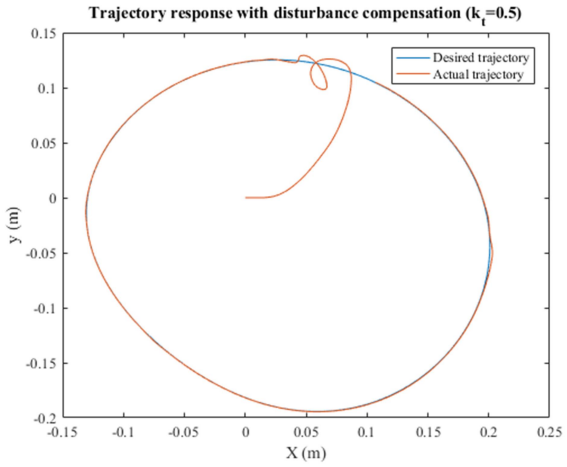

Fig. 9. Trajectory response with disturbance compensation with high k_t

7. Conclusion

This paper introduces a stable virtual sensor based on second order sliding modes. This virtual sensor is used for feedback linearization of the nonlinear model of the delta robot. It assumes that the robot model is unknown, it requires only the measured joint position. The convergence and stability are proven based on Lyapunov function. The estimated disturbance is added to the control law through an adaptively tuned gain to decrease the effect of the transient response of the estimation on the control signal. The results confirmed that this proposed sensor is stable and converges in finite time, further, the control approach decreases the tracking error to zero.

References

[1] I. Hashlamon and K. Erbatur, "Joint sensor fault detection and recovery based on virtual sensor for walking legged robots," in *IEEE 23rd International Symposium on Industrial Electronics*, Istanbul, 2014, pp. 1210-1214.

[2] I. Hashlamon and K. Erbatur, "Simple Virtual Slip Force Sensor for walking biped robots," in *9th AsianControl Conference (ASCC),* , Istanbul, 2013, pp. 1-5.

[3] Q. Ahmed, A. I. Bhatti, and M. Iqbal, "Virtual Sensors for Automotive Engine Sensors Fault Diagnosis in Second-Order Sliding Modes," *Sensors Journal, IEEE,* vol. 11, pp. 1832-1840, 2011.

[4] G. Heredia and A. Ollero, "Virtual Sensor for Failure Detection, Identification and Recovery in the Transition Phase of a Morphing Aircraft," *Sensors,* vol. 10, pp. 2188-2201, 2010.

[5] E. Villagrossi, L. Simoni, M. Beschi, N. Pedrocchi, A. Marini, L. M. Tosatti*, et al.*, "A virtual force sensor for interaction tasks with conventional industrial robots," *Mechatronics,* vol. 50, pp. 78-86, 2018.

[6] E. Magrini, F. Flacco, and A. De Luca, "Estimation of contact forces using a virtual force sensor," in *IEEE/RSJ International Conference on Intelligent Robots and Systems*, 2014, pp. 2126-2133.

[7] M. Dyck and M. Tavakoli, "Measuring the dynamic impedance of the human arm without a force sensor," in *IEEE 13th International Conference on Rehabilitation Robotics (ICORR)*, 2013, pp. 1-8.

[8] A. Zidan, D. Kaczor, S. Tappe, and T. Ortmaier, "Optimization of a P/PI Cascade Motion Controller for a 3-DOF Delta Robot," in *Tagungsband des 4. Kongresses Montage Handhabung Industrieroboter*, ed: Springer, 2019, pp. 217-226.

[9] L. Angel, J. Sebastian, R. Saltaren, and R. Aracil, "RoboTenis system part II: Dynamics and control," in *Proceedings of the 44th IEEE Conference on Decision and Control*, 2005, pp. 2030-2034.

[10] J. Fabian, C. Monterrey, and R. Canahuire, "Trajectory tracking control of a 3 DOF delta robot: a PD and LQR comparison," in *IEEE International Congress onElectronics, Electrical Engineering and Computing (INTERCON)*, 2016, pp. 1-5.

[11] A. Dumlu and K. Erenturk, "Trajectory tracking control for a 3-dof parallel manipulator using fractional-order PI^lambda {D}^mu control," *IEEE Transactions on Industrial Electronics,* vol. 61, pp. 3417-3426, 2013.

[12] Y.-L. Kuo and P.-Y. Huang, "Experimental and simulation studies of motion control of a Delta robot using a model-based approach," *International Journal of Advanced Robotic Systems,* vol. 14, pp. 1-14, 2017.

[13] K. P. Jankowski and H. Van Brussel, "An approach to discrete inverse dynamics control of flexible-joint robots," *IEEE Transactions on Robotics and Automation,* vol. 8, pp. 651-658, 1992.

[14] Y. Su, D. Sun, L. Ren, and J. K. Mills, "Integration of saturated PI synchronous control and PD feedback for control of parallel manipulators," *IEEE Transactions on Robotics,* vol. 22, pp. 202-207, 2006.

[15] H.-H. Lin, Y.-H. Ta, and C.-S. Liu, "The implementation of smoothing robust control for a delta robot," in *Second International Conference on Robot, Vision and Signal Processing*, 2013, pp. 208-213.

[16] C. E. Boudjedir, D. Boukhetala, and M. Bouri, "Nonlinear PD plus sliding mode control with application to a parallel delta robot," *Journal of Electrical Engineering,* vol. 69, pp. 329-336, 2018.

[17] C. Lu, X. Miao, S. Wang, and C. Zhang, "Research on Adaptive Robust Control Algorithm for Delta Parallel Robots," Singapore, 2019, pp. 59-68.

[18] L. Angel and J. Viola, "Fractional order PID for tracking control of a parallel robotic manipulator type delta," *ISA transactions,* vol. 79, pp. 172-188, 2018.

[19] J. Kardoš, "Robust Computed Torque Method of Robot Tracking Control," in *International Conference on Process Control (PC19)*, 2019, pp. 102-107.

[20] J. Davila, L. Fridman, and A. Levant, "Second-order sliding-mode observer for mechanical systems," *Automatic Control, IEEE Transactions on,* vol. 50, pp. 1785-1789, 2005.

[21] V. I. Utkin, *Sliding modes in control and optimization*: Springer Science & Business Media, 2013.

[22] I. Boiko, L. Fridman, and M. Castellanos, "Analysis of second-order sliding-mode algorithms in the frequency domain," *IEEE Transactions on Automatic Control,* vol. 49, pp. 946-950, 2004.

[23] A. Levant, "Principles of 2-sliding mode design," *automatica,* vol. 43, pp. 576-586, 2007.

[24] J. A. Moreno and M. Osorio, "A Lyapunov approach to second-order sliding mode controllers and observers," in *IEEE Conference onDecision and Control* 2008, pp. 2856-2861.

[25] F. Pierrot, C. Reynaud, and A. Fournier, "DELTA: a simple and efficient parallel robot," *Robotica,* vol. 8, pp. 105-109, 1990.

[26] L. Yan, D. Liu, and Z. Jiao, "Novel design and kinematics modeling for delta robot with improved end effector," in *IECON - 42nd Annual Conference of the IEEE Industrial Electronics Society*, 2016, pp. 741-746.

[27] J. Brinker, B. Corves, and M. Wahle, "A comparative study of inverse dynamics based on clavel's delta robot," in *Proceedings of the 14th World Congress in Mechanism and Machine Science*, Taipei, Taiwan, 2015, pp. 25-30.

[28] A. Olsson, "Modeling and control of a Delta-3 robot," Master Department of Automatic Control, Lund University, 2009.

[29] A. Vivas, P. Poignet, F. Marquet, F. Pierrot, and M. Gautier, "Experimental dynamic identification of a fully parallel robot," in *IEEE International Conference on Robotics and Automation* 2003, pp. 3278-3283.

[30] C. G. R. Paraponiaris, "A method for the mechatronico analysis of parallel kinematics manipulators based on decoupling the dynamics of actuators and mechanism," Ph.D., Department of Mechanical Engineering, University of the Basque Country, 2017.

[31] M. López, E. Castillo, G. García, and A. Bashir, "Delta robot: inverse, direct, and intermediate Jacobians," *Proceedings of the Institution of Mechanical Engineers, Part C: Journal of Mechanical Engineering Science,* vol. 220, pp. 103-109, 2006.

[32] T. Su, L. Cheng, Y. Wang, X. Liang, J. Zheng, and H. Zhang, "Time-optimal trajectory planning for Delta robot based on quintic pythagorean-hodograph curves," *IEEE Access,* vol. 6, pp. 28530-28539, 2018.

[33] R. Hayat, M. Leibold, and M. Buss, "Robust-Adaptive Controller Design for Robot Manipulators Using the H_infinity Approach," *IEEE Access,* vol. 6, pp. 51626-51639, 2018.

[34] I. Hashlamon and K. Erbatur, "Reduced Filtered Dynamic Model for Joint Friction Estimation of Walking Bipeds," *Jordan Journal of Mechanical & Industrial Engineering,* vol. 11, 2017.

[35] I. Hashlamon and K. Erbatur, "Joint friction estimation for walking bipeds," *Robotica,* vol. 34, pp. 1610-1629, 23/9/2014 2014.

[36] J. Cortes, "Discontinuous dynamical systems: a tutorial on solutions, nonsmooth analysis, and stability," *arXiv preprint arXiv:0901.3583,* 2009.

[37] C. Makkar, W. E. Dixon, W. G. Sawyer, and G. Hu, "A new continuously differentiable friction model for control systems design," in *IEEE/ASME International Conference on Advanced Intelligent Mechatronics*, Monterey, CA, 2005, pp. 600-605.